Available online at www.sciencedirect.com
ScienceDirect
Russian Geology and Geophysics 51 (2010) 708–718
RUSSIAN GEOLOGY AND GEOPHYSICS
www.elsevier.com/locate/rgg

Inversion of IP-affected TEM responses of a two-layer earth

N.O. Kozhevnikov *, E.Yu. Antonov

A.A. Trofimuk Institute of Petroleum Geology and Geophysics, Siberian Branch of the Russian Academy of Sciences, prosp. Akad. Koptyuga 3, Novosibirsk, 630090, Russia

Received 17 February 2009; received in revised form 21 October 2009; accepted 16 November 2009

Abstract

A numerical experiment has been applied to explore the potentialities and the limitations of the inversion of IP-affected TEM responses of a two-layer earth with a polarizable layer above (Model 1) or below (Model 2) a nonpolarizable layer. The IP effects have been incorporated into the models via a Cole–Cole complex frequency-dependent conductivity. One of us computed synthetic in-loop and coincident-loop transient responses with added Gaussian noise, and the other performed single and joint inversion of the two sets of pseudo-experimental data. Model 1 turns out to be advantageous over Model 2 in TEM applications and gives a good fit of the Cole–Cole parameters (chargeability, IP time constant, and exponent) even in the absence of a priori information. In the case of Model 2, the lack of a priori information causes problems as to recognize which layer is polarizable, and the fit of the Cole–Cole parameters is generally worse. The layer thicknesses and resistivities are rather accurate in both groups of models, irrespective of whether a priori information is available. As the upper layer increases in thickness (H_1), the fit of its parameters ever improves in both models while the parameters of the lower layer, on the contrary, contain a greater error. Joint inversion of in-loop and coincident-loop transients improves the fit in most cases.

Relative rms error (σ_{rel}) does not depend on the upper layer thickness for Model 1 but decreases as H_1 increases in the case of Model 2. The error in joint inversion is times that in single inversion, which means that additional criteria other than σ_{rel} may be useful to estimate the inversion quality.

Keywords: TEM method; induced polarization; inversion; frozen ground

Introduction

Processing transient responses affected by fast-decaying induced polarization (IP) is an important problem (Kamenetskii et al., 1990; Svetov et al., 1996) to be solved with both field and numerical experiments. There are, however, no geological objects documented in situ to a resolution sufficient for a systematic and explicit study of the transient process as a function of loop configuration and IP patterns. Thus, simulation with specially organized numerical experiments is the only appropriate way of looking into IP effects on transient responses.

In our previous papers (Kozhevnikov and Antonov, 2007, 2008, 2009a) we discussed numerical experiments exploring the potentialities and limitations in the inversion of IP-affected responses of a uniform conductive earth. The uniform-earth assumption is suitable for any complex of rocks, uniform in polarizability and conductivity, with a size at least several times the loop size. Yet, the uniform-halfspace approximation is not always workable. Therefore, in this study we are making another step towards the reality by proceeding to a layered-earth assumption.

Choice of models and their general characteristics

Two-layer models (Fig. 1) are as fundamental among layered models as those of a uniform earth among all geoelectirc models. The two-layer approximation is suitable for many basic problems of layered halfspace and, at the same time, with relatively few parameters, is simple enough to analyze and interpret both forward and inverse solutions. On the other hand, it is good to simulate many important geological objects, such as bedrock buried under sediments, active layer with seasonally frozen ground upon a thaw or a thaw upon frozen ground, lavas lying over a thick uniform sequence of other rocks, etc.

In the reported experiments we focused on two specific but essential two-layer cases: (i) a polarizable layer above and a nonpolarizable layer below (Model 1) and (ii) a nonpolarizable layer above and a polarizable layer below (Model 2).

* Corresponding author.
E-mail address: KozhevnikovNO@ipgg.nsc.ru (N.O. Kozhevnikov)

1068-7971/$ - see front matter © 2010, V.S. Sabolev IGM, Siberian Branch of the RAS. Published by Elsevier B.V. All rights reserved.
doi:10.1016/j.rgg.2010.05.011

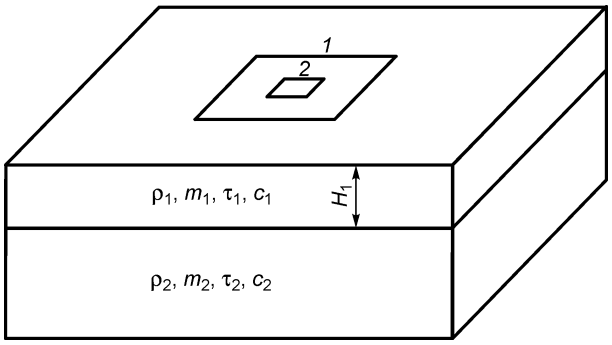

Fig. 1. Experiment layout: transmitter (*1*) and receiver (*2*) loops on a two-layer polarizable conducting earth.

That choice was not fortuitous. Since the late 1970s–early 1980s, TEM-related publications on western Yakutia have contained ever more reports of monotony break or sign reversal in signals (Molchanov and Sidorov, 1985; Sidorov, 1985). The nonmonotonous responses were observed at times from a few tens to a few hundreds of milliseconds and were originally thought of as noise. Rather soon, however, they were understood to result from fast decaying induced polarization (Molchanov and Sidorov, 1985; Sidorov, 1985, 1987) which can be incorporated in modeling, at least in a formal way, via the Cole–Cole complex frequency-dependent conductivity $\sigma^*(\omega)$ (Wait, 1982):

$$\sigma^*(\omega) = \sigma_0 \frac{1 + (j\omega\tau)^c}{1 + (1 - m)(j\omega\tau)^c} \quad (1)$$

where $j = \sqrt{-1}$; ω is the angular frequency, in s^{-1}; σ_0 is the dc conductivity, in S/m; m is the chargeability, $(0 \le m \le 1)$; c is the exponent; τ is the IP relaxation time constant, in s.

The origin of fast-decaying IP in western Yakutia has been a subject of controversy. One hypothesis most explicitly formulated by Mityukhin (1985) attributes the sign reversal in transients from the Malaya Botuobiya region to polarizability of terrigenous-carbonate sediments of the Late Cambrian Ilga Formation associated with high contents of reduced iron sulfide. The high concentration of reduced iron in the vicinities of the known kimberlite and tuff pipes may, in turn, be a consequence of specific host-rock chemistry, with reduction being maintained by hydrogen sulfide input from deeper sedimentary strata. The hypothesis found more support later in (Zhandalinov, 2005).

An alternative idea is that the nonmonotonous responses record frequency-dependent conductivity of *frozen* ion-conducting ground (Artemenko and Kozhevnikov, 1999; Karasev et al., 2004; Kozhevnikov and Antonov, 2006; Kozhevnikov and Artemenko, 2004; Kozhevnikov et al., 1995; Krylov and Bobrov, 2002; Molchanov and Sidorov, 1985; Shesternev et al., 2003; Stognii, 2008; Zadorozhnaya and Lepeshkin, 1998), though the many partisans of this hypothesis disagree about the very mechanism of frequency dependence.

The recently appeared tools for processing IP-affected transient responses may shed light on the causes of fast-decaying polarization in western Yakutia. If the former idea is true, polarizable rocks must be buried, otherwise it is the upper section that must be polarized due to its coldest temperature, ice contents, dispersive material, etc. To put it different, by indicating the position of the polarizable layer either above or below, the inversion of IP-affected transients will furnish evidence, respectively, for the frozen ground or sulfide mineralization hypotheses. Preliminary 1D inversion of IP-affected TEM responses from a kimberlite field in western Yakutia reported in (Kozhevnikov and Antonov, 2006) showed polarizability of ion-conducting frozen shallowest sediments. Stognii (2008) arrived at a similar inference having inverted data acquired with different loop geometries using the Cole–Cole frequency-dependent conductivity and thus having obtained models that took into account both geology and cryology.

Those results are important but are neither exhaustive nor final in the sense that the potentialities and limitations in the inversion of transient responses of a two-layer earth remain unclear. That was specifically the motivation of our numerical experiments and the choice of models with certain Cole–Cole parameters.

Many areas in western Yakutia explored for kimberlites have the upper section consisting of Jurassic clay and sand from a few meters to 100 m thick or thicker. The clayey sediments, even being frozen, have low resistivities (ρ_1) rarely exceeding tens or a few hundreds of Ohm · m. Jurassic sediments lie over Paleozoic carbonate-terrigenous rocks with their resistivities (ρ_2) about 10^3 Ohm · m (if they are free from conductive mineralized fluid).

The chargeability m_1 of thaw sand-clay deposits is about zero but can reach a few tenths if the rocks are frozen (Krylov and Bobrov, 2002; Olenchenko et al., 2008; Shesternev et al., 2003). The chargeability m_2 of frozen sulfide-impregnated carbonate sediments is poorly known but may be inferred to be within 0.2–0.3 from data in (Mityukhin, 1985; Pelton et al., 1978; Zhandalinov, 2005). Proceeding from the experience of processing TEM data from western Yakutia, one may assume the relaxation time constant τ to be tens of microseconds and the exponent c to be about 1.

Therefore, the parameters were chosen as ρ_1 = (50–200) Ohm · m, m_1 = 0.05–0.25, $\tau_1 = (2 \cdot 10^{-5}–1.5 \cdot 10^{-4})$ s, c_1 = 0.8–1, ρ_2 = (500–2000) Ohm · m, m_2 = 0 for Model 1, and ρ_1 = (50–200) Ohm · m, m_1 = 0, ρ_2 = (500–2000) Ohm · m, m_2 = 0.05–0.25, $\tau_2 = (2 \cdot 10^{-5}–1.5 \cdot 10^{-4})$ s, and c_2 = 0.8–1 for Model 2. The layer thickness H_1 was thus assumed to be in the range 1–200 m as in nature it may vary from zero (when carbonate rocks are exposed) to 100 m or more.

Numerical experiments

The numerical experiments were carried out following the procedure reported in (Kozhevnikov and Antonov, 2007, 2008,

2009a). One of us (N. Kozhevnikov) computed synthetic transients and the other (E. Antonov) inverted the generated pseudo-experimental responses in terms of a layered polarizable earth.

The inversion quality was investigated using five starting ("true") models of group 1 (Model 1, Table 1) and seven models of group 2 (Model 2, Table 2), with parameters selected from the above ranges. The choice of parameters was made random in order to avoid interpreter's personal biases toward a "good" set (at which the success of inversion would be more certain).

For generating the synthetic IP-affected responses and their single and joint inversion, we used the Inv_QQIP and JInv_QQIP software designed by E.Yu. Antonov at IPGG (Novosibirsk).

In order to see how the inversion quality depends on loop configuration and to assess the potentialities of joint inversion of data from different arrays, the transients were computed for an in-loop (200 m × 200 m transmitter and 50 m × 50 m receiver) and a 50 m × 50 m coincident-loop configurations. External random noise and instrumental errors common to field measured transients were simulated by imposing noise on the synthetic transients as a generated Gaussian series of random numbers.

The time range of the generated transients was defined by the loop size and instrumental facilities. The delay times started at 10–30 μs because, according to the field experience, the transient processes induced by the TEM system response decay at 10 μs and 30 μs for 50 m × 50 m and 200 m × 50 m loops, respectively. The latest delay time was 100 ms for all synthetic responses; the times used in inversion depended on models resistivities but extended to no more than 1.3 ms for the 50 m × 50 m loop and 6 ms for the 200 m × 50 m loop. Those values corresponded to the limit where the responses were of the order of less than 0.1 μV.

As before, in the case of a single loop size, the inverse problem was solved by fitting a set of parameters from the model data space to the minimum of the goal function $\varphi(\mathbf{P})$:

$$\varphi(\mathbf{P}) = \left\{ \frac{1}{N-1} \sum_{i=1}^{N} \left[\frac{\varepsilon^{\exp}(t_i) - F_{\mathbf{P}}(t_i)}{\delta(t_i)\varepsilon^{\exp}(t_i)} \right]^2 \right\}^{1/2} \quad (2)$$

where t_i is the ith time delay, N is the total number of time delays; $F_{\mathbf{P}}$ is the forward operator; $\delta(t_i)$ is the relative measurement error at the delay t_i. The set of model parameters is the vector $\mathbf{P} = (\sigma_j, h_j, m_j, \tau_j, c_j)\Big|_{j=1,M}$ where M is the total number of layers, σ_j is the conductivity, h_j is the layer thickness, m_j is the chargeability, τ_j is the IP time constant, and c_j is the exponent for the jth layer. Functional (2) was minimized using a modified algorithm by Nelder and Mead (1965).

Joint inversion differed from single inversion in that the goal function equation included data for both loop configurations, i.e., $N = N_1 + N_2$, where N_1, is the number of delays and corresponding voltages for one and N_2 is that for the other system. Unlike the single inversion, the synthetic transients of the two systems were calculated using forward runs with regard to each loop configuration. To put it different, the total forward operator $F_{\mathbf{P}}$ comprised the operators $F_{\mathbf{P}1}$ and $F_{\mathbf{P}2}$, for the 200 m × 50 m in-loop and 50 m × 50 m coincident-loop responses, respectively. The measurement errors $\delta(t_i)$ included in (2) were different in the two systems, and the errors in joint inversion were thus assumed to be 2% at $1 \le i \le N_1$ and 5% at $N_1 + 1 \le i \le N$.

Results

Model 1. The interpreter (E. Antonov) received generated transients corresponding to Model 1 (polarizable upper layer and nonpolarizable lower layer) and inverted them being totally unaware of the model to be inverted, but the form of the responses prompted a guess that it was a two-layer earth. Inversion began with the 50 m × 50 m coincident-loop responses, then fitting was applied to the 200 m × 50 m in-loop data, and, finally, both data sets were inverted jointly. As a result of both single and joint inversion procedures, all five models were identified to represent a section with a polarizable layer above and a nonpolarizable layer below.

We investigated the inversion quality using normalized parameters (Fig. 2). Assuming some Cole–Cole parameter to be independent and plotting it against normalized values of the respective fitted parameter (Kozhevnikov and Antonov, 2007) helps avoiding problems in imaging the inversion

Table 1. Parameters of true models, with polarizing upper layer and nonpolarizing lower layer (Model 1)

Model	H_1, m	ρ_1, Ohm · m	m_1	τ_1, s	c_1	ρ_2, Ohm · m
1	1	100	0.1	$5 \cdot 10^{-5}$	1	1000
2	2	200	0.1	$5 \cdot 10^{-5}$	0.9	500
3	10	100	0.05	$5 \cdot 10^{-5}$	1	1000
4	50	50	0.2	$1 \cdot 10^{-4}$	0.95	2000
5	200	200	0.1	$2.5 \cdot 10^{-5}$	0.9	1000

Table 2. Parameters of true models, with nonpolarizing upper layer and polarizing lower layer (Model 2)

Model	H_1, m	ρ_1, Ohm · m	ρ_2, Ohm · m	m_2	τ_2, s	c_2
1	1	150	1500	0.1	$3 \cdot 10^{-5}$	0.9
2	2	100	1000	0.25	$5 \cdot 10^{-5}$	0.95
3	5	100	600	0.2	$1.5 \cdot 10^{-4}$	1
4	10	50	1250	0.125	$5 \cdot 10^{-5}$	1
5	20	60	1000	0.075	$4 \cdot 10^{-5}$	0.8
6	50	125	800	0.05	$7.5 \cdot 10^{-5}$	1
7	100	80	2000	0.1	$2 \cdot 10^{-5}$	0.95

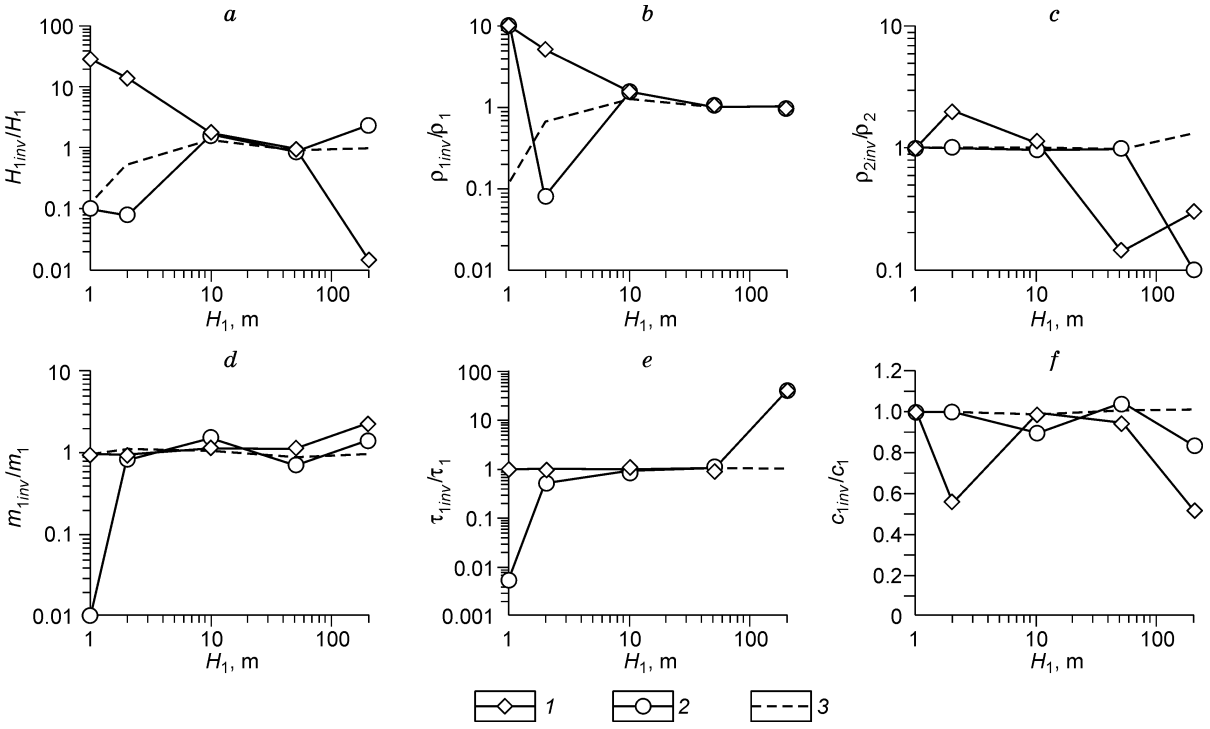

Fig. 2. Parameters reproduced in single and joint inversion (Model 1) as a function of thickness H_1: H_{1inv} (*a*), ρ_{1inv} (*b*), ρ_{2inv} (*c*), m_{1inv} (*d*), τ_{1inv} (*e*), c_{1inv} (*f*), in absence of a priori information. *1*, coincident-loop configuration; *2*, in-loop configuration; *3*, joint inversion.

results. In our case, the layer thickness H_1 appears to be a good candidate for an independent parameter. Thus, to present the data in an easily readable way, the *y* axis in Fig. 2 shows the normalized values of the fitted parameters. H_1, ρ_1, m_1, τ_1, c_1, and ρ_2 (Fig. 2) are the "true" parameters (i.e., those assumed in computing pseudo-experimental transients) while H_{1inv}, ρ_{1inv}, m_{1inv}, τ_{1inv}, c_{1inv}, and ρ_{2inv} are those obtained through inversion; their ratios H_{1inv}/H_1, ρ_{1inv}/ρ_1, m_{1inv}/m, τ_{1inv}/τ, c_{1inv}/c, ρ_{2inv}/ρ_2 measure relative deviation of the fitted parameters from the true ones.

We varied the H_{1inv}/H_1 ratio trying different layer thicknesses (Fig. 2, *a*). Single inversion in the cases of a thin ($H_1 <$ 10 m) and a thick ($H_1 > 50$ m) upper layer led to large H_1 errors, and joint inversion was obviously efficient ($H_{1inv} = H_1$) at the thicknesses from 2 to 200 m.

The resistivity ρ_1 of the upper layer (Fig. 2, *b*) derived by single inversion showed a good fit at $H_1 \geq 10$ m. At smaller H_1, the quality of joint inversion was notably better: the difference between the resistivity ρ_{1inv} and ρ_1 was no more than 30–40% already at $H_1 = 2$ m.

The chargeability (m_1) estimates (Fig. 2, *d*) were rather accurate in single inversion, especially, of the coincident-loop data, while joint inversion made the result really excellent: $m_{1inv}/m_1 = 1$ at any H_1.

As for the IP time constant τ_1 (Fig. 2, *e*), the $\tau_{1inv} - \tau_1$ misfit was large in single inversion (at $H_1 = 1$ m for the in-loop system and $H_1 = 200$ m for both configurations), but the quality of joint inversion was perfect ($\tau_{1inv}/\tau_1 = 1$) at any upper layer thickness.

The single inversion-derived exponent c_1 (Fig. 2, *f*) was either notably different from or similar to the true value depending on the loop geometry and H_1. An unexpected result was that the deviation of c_{1inv}/c_1 from the unity in the case of coincident-loop responses turned out to be greater than in the in-loop case. Joint inversion, however, gave $c_{1inv} = c_1$ irrespective of H_1.

The resistivity of the lower layer found by single inversion (ρ_{2inv}) approached ρ_2 at small H_1 thicknesses (Fig. 2, *c*), and the error increased for almost an order of magnitude at H_1 above 10 m (in the coincident-loop case) or 50 m (in the in-loop case). Yet, joint inversion was of excellent quality throughout the H_1 range.

Summing up, we stress first of all that even without a priori information, the interpreter correctly identified the two-layer pattern with a polarizable upper layer and a nonpolarizable lower layer. The general inversion quality was evaluated as a ratio of the number of correctly determined parameters to the total number of parameters (five models with six parameters in each, i.e., thirty parameters altogether). With this approach, single inversion was 65–70% positive for each loop geometry, and joint inversion gave correct estimates in 90% of cases. That is why we found it pointless to continue the experiment by communicating the interpreter more pieces of a priori information, i.e., the inversion problem was assumed to have been resolved.

Model 2. Unlike the case of Model 1, the inversion procedure with Model 2 (a nonpolarizable layer above and a polarizable layer below) included several stages, namely:

(1) inversion without a priori information (E. Antonov, the interpreter, was totally unaware of the true models);

(2) inversion with a priori information (E. Antonov, the interpreter, was told that the polarizable layer was below);

(3) inversion with additional a priori information (in addition to (2), E. Antonov, the interpreter, knew the thickness of the upper layer).

Stage 1. Although each of the seven models was correctly identified as a two-layer one, polarizability was inferred either for the upper or the lower layer, or for both, depending on combinations of the parameters and loop configurations. Thus, the inversion quality turned out to be uneven and the results were hard to systematize and to present using normalized parameters as in Fig. 2. Therefore, below we report the inversion results for three typical cases of a nonpolarizable upper layer of large, medium, and small thicknesses (Fig. 3).

Figure 3 (*a–c*) shows "true" depth-dependent chargeabilities for H_1 = 1, 5, and 50 m, respectively (Nos. 1, 3, 6, Model 2, Table 2), with the corresponding IP time constants and exponents (on the left), and those obtained by single and joint inversion (on the right).

The plots of depth-dependent chargeability were made in log-log to allow for the large variability. The depth was allowed to vary from 0.001 m (in essence, the halfspace with the parameters of the lower layer) to 1000 m (in essence, the halfspace with the parameters of the upper layer), and the chargeability range was from 0.01 (almost nonpolarizable medium) to 1.0.

Before proceeding to comments on Fig. 3 we note that an inversion-derived model with the upper layer (H_1) much thinner than the loop size can be treated as a uniform earth with the parameters of the lower layer and, vice versa, a two-layer model with the upper layer thicker than the loop size, is, in terms of survey practice, a uniform earth with the parameters of the upper layer. We discussed this approach in detail in (Kozhevnikov and Antonov, 2007, 2009a).

The inversion results in the case of a thin upper layer (H_1 = 1 m, Fig. 3, *a*) were as follows. Single inversion of in-loop transients led to a uniform polarizable earth. Although the uniform-earth approximation was acceptable in that case, the chargeability, the time constant, and the exponent were reproduced to a large error. Single inversion of coincident-loop data yielded a polarizable upper layer of the thickness H_{1inv} = 23 m with the Cole–Cole parameters similar to those of the true model: m_{1inv} = 0.16, τ_{1inv} = 31 μs, c_{1inv} = 0.78. Joint inversion again gave an excellent fit.

With a thicker upper layer (H_1 = 5 m, Fig. 3, *b*), its influence was no more negligible. Inversion of generated in-loop transients led to a model with a 8.5 m thick polarizable upper layer. Although the position of the polarizable layer was wrong, the Cole–Cole parameters (m_{1inv} = 0.21, τ_{1inv} = 150 μs, and c_{1inv} = 0.98) were very close to the "true" ones. The model obtained by inversion of coincident-loop transients faithfully reproduced the true model. The results of joint inversion were almost the same as in the single inversion of in-loop transients: the starting Cole–Cole parameters were reproduced to a good accuracy but the upper layer rather than the lower one appeared polarizable.

Finally, with a thick upper layer (H_1 = 50 m, Fig. 3, *c*), both single and joint inversion gave models with a polarizable lower layer and $H_{1inv} = H_1$. However, the fit of the Cole–Cole parameters was generally poor, except for chargeability in joint inversion (m_{2inv} = 0.07 against m_2 = 0.05).

Figure 3 provides an idea of how the inversion models fit the two-layer models with a nonpolarizable lower layer and how the chargeability, the time constant, and the exponent fit the respective parameters of the true models. As for the fit of resistivities (ρ_{1inv} and ρ_{2inv}) and upper layer thicknesses (H_{1inv}), it is better to judge in the plots of the ratios ρ_{1inv}/ρ_1, ρ_{2inv}/ρ_2, H_{1inv}/H_1 as a function of H_1 (Fig. 4). Besides the resistivity and layer thickness, Fig. 4, *c* shows the fit of conductance as $S_{1inv}/S_1 = f(H_1)$, where $S_1 = H_1/\rho_1$.

The inversion-derived layer thickness is obviously overestimated by a factor of several tens to thousands at small H_1 (Fig. 4, *a*) but the inversion quality improves rapidly as it increases: H_{1inv} is almost identical to H_1 at $H_1 \geq 5$ m (Fig. 4, *a*). The same holds for the resistivity ρ_{1inv} (Fig. 4, *b*): $\rho_{1inv}/\rho_1 \approx 10$ at $H_1 < 5$ m but $\rho_{1inv} = \rho_1$ at $H_1 \geq 5$ m. The predicted resistivity of the lower layer ρ_{2inv} (Fig. 4, *d*) practically does not depend on the upper layer thickness: as H_1 changes from 1 to 100 m (i.e., 100 times), the $\rho_{2inv} - \rho_2$ difference is no more than 30% (15% on average). The conductance approaches the true value already at $H_1 \geq 2$ m (Fig. 4, *c*)

Single inversion for H_{1inv}, ρ_{1inv}, S_{1inv}, and ρ_{2inv} turned out to be so good that joint inversion could not improve the result significantly (Fig. 4).

Thus, the results of Stage 1 of the experiment when the interpreter did not have any prior information can be summarized as follows. In all cases the models were identified as two-layer ones but the lower layer was recognized to be polarizable only when the conducting layer was thin enough. The fit of the Cole–Cole parameters m_{2inv}, τ_{2inv}, and c_{2inv} was good if the upper layer was no thicker than 5–10 m but worsened as H_1 increased. The fit of the resistivity, thickness, and conductivity of the upper layer was good at H_1 thicker than 5 m; the resistivity of the lower layer showed a perfect fit ($\rho_{2inv}/\rho_2 \approx 1$) at any H_1 from 1 to 100 m.

Stage 2. Single and joint inversion at Stage 2 of the experiment (Fig. 5) predicted the thickness of the upper layer to a large error if it was thin (Fig. 5, *a*), like in the case of Stage 1, but already at H_1 = 2 m the error in joint inversion reduced to a few tens of percent. A good layer thickness fit was achieved at $H_1 \geq 10$ m in single inversion and at $H_1 >$ 2 m in joint inversion. The results were the same for the upper layer resistivity (Fig. 5, *b*); the resistivity of the lower layer (Fig. 5, *c*) was reproduced to a satisfactory accuracy in single inversion and to a perfect accuracy in joint inversion, at any thickness of the upper layer.

The chargeability, time constant, and exponent estimates (Fig. 5, *d–f*) were of a satisfactory fit if the upper layer was rather thin ($H_1 <$ 10–20 m) but the misfit increased markedly in the case of a thicker H_1: one or two orders of magnitude

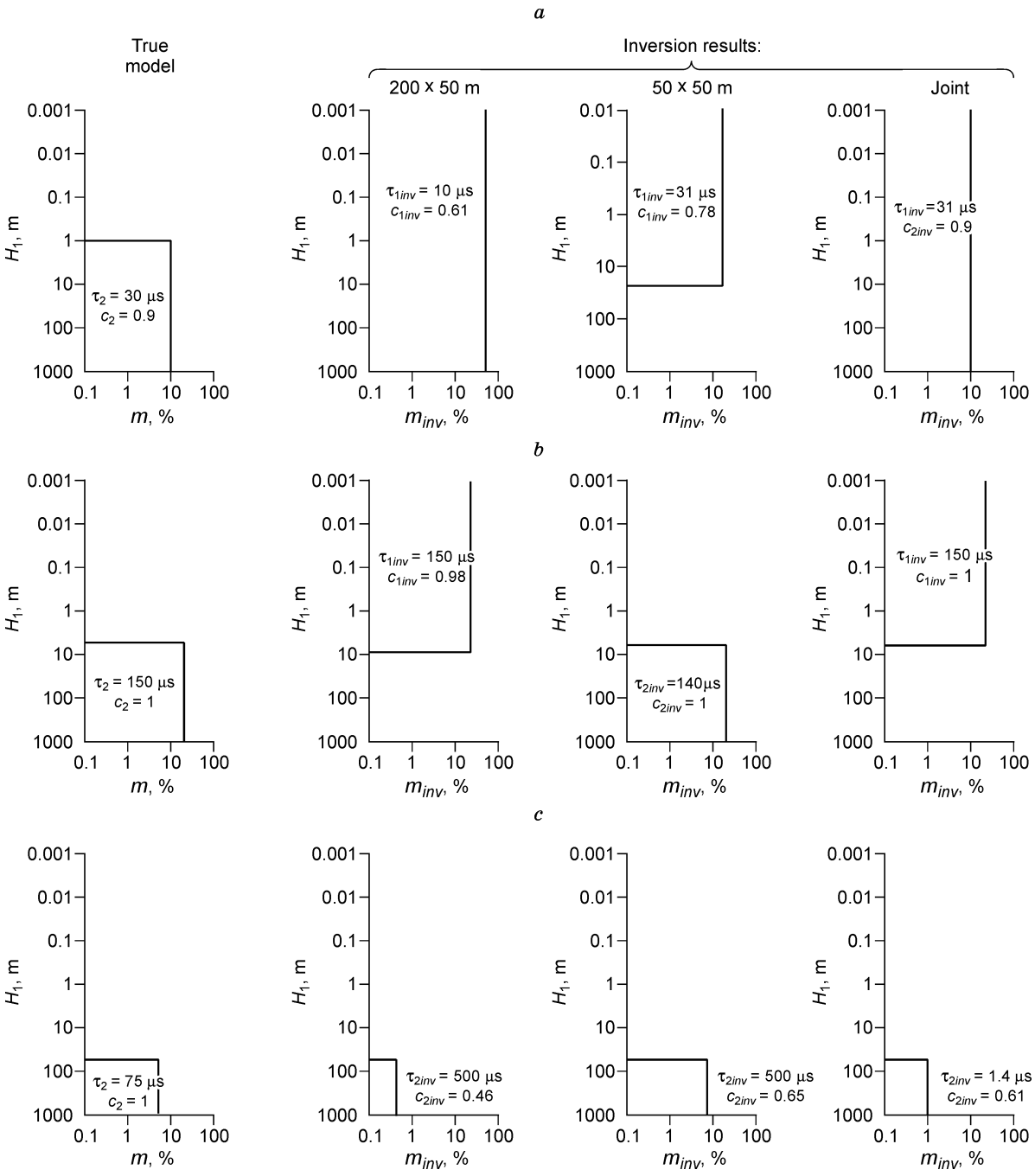

Fig. 3. True models and results of single and joint inversion. H_1 = 1 m (*a*), H_1 = 5 m (*b*), H_1 = 50 m (*c*).

for chargeability and two orders of magnitude for relaxation time. Joint inversion improved the chargeability estimates but was of a poor quality at H_1 = 100 m (Fig. 5, *d*, *e*).

Thus, the Cole–Cole parameters of the upper layer were reproduced worse than those of the lower layer at small H_1 but the situation changed to the opposite when H_1 increased. The resistivity of the lower layer predicted by single and, especially, joint inversion was close to the true values at any upper layer thickness.

Stage 3. The inversion results of Stage 3 are presented in Fig. 6 in the same way as in Figs. 2 and 5. The results, as well as the corresponding conclusions, are generally similar to those of Stage 2, i.e., the a priori knowledge of the layer thickness did not improve much the inversion quality. The chargeability of the lower layer at $H_1 \geq 10$ m turned out to be even less accurate than in the previous case (Figs. 5, *d* and 6, *d*). Yet, the fit of the time constant was better, especially in joint inversion (Figs. 5, *e* and 6, *e*).

Thus, knowing the upper layer thickness did not help much: the fit was better than at Stage 2 for the time constant but worse for the chargeability, i.e., joint inversion was advantageous only as to the relaxation time (Fig. 6, *e*).

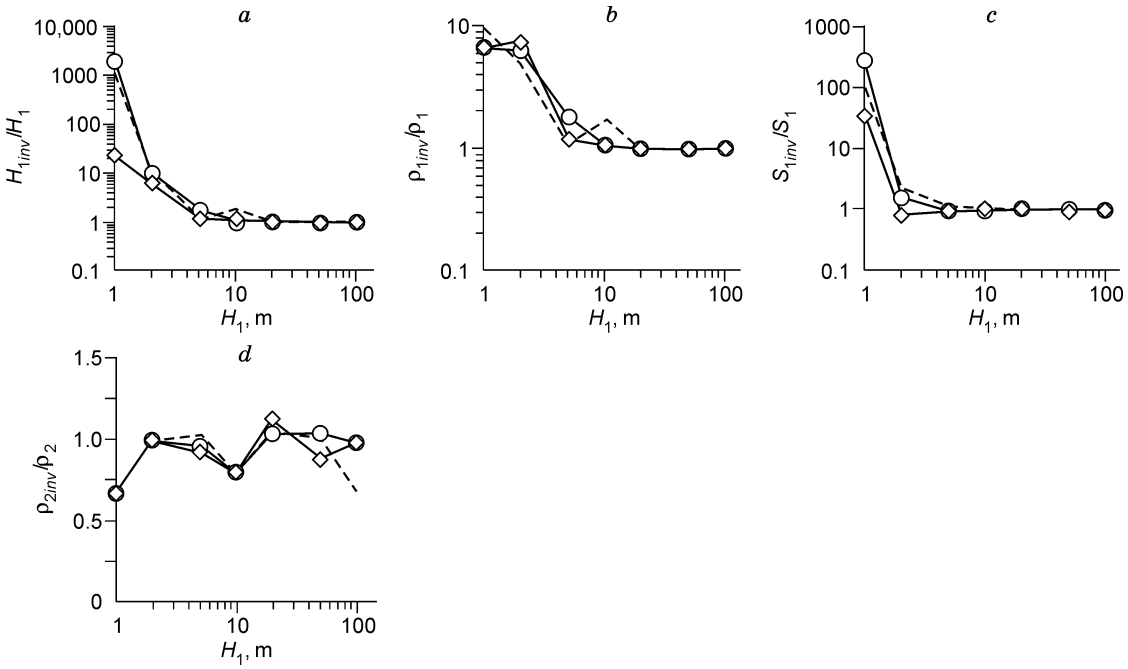

Fig. 4. Parameters reproduced in single and joint inversion (Model 2) as a function of thickness H_1: H_{1inv} (*a*), ρ_{1inv} (*b*), S_{1inv} (*c*), ρ_{2inv} (*d*). No a priori information available (Stage 1). Symbols same as in Fig. 2.

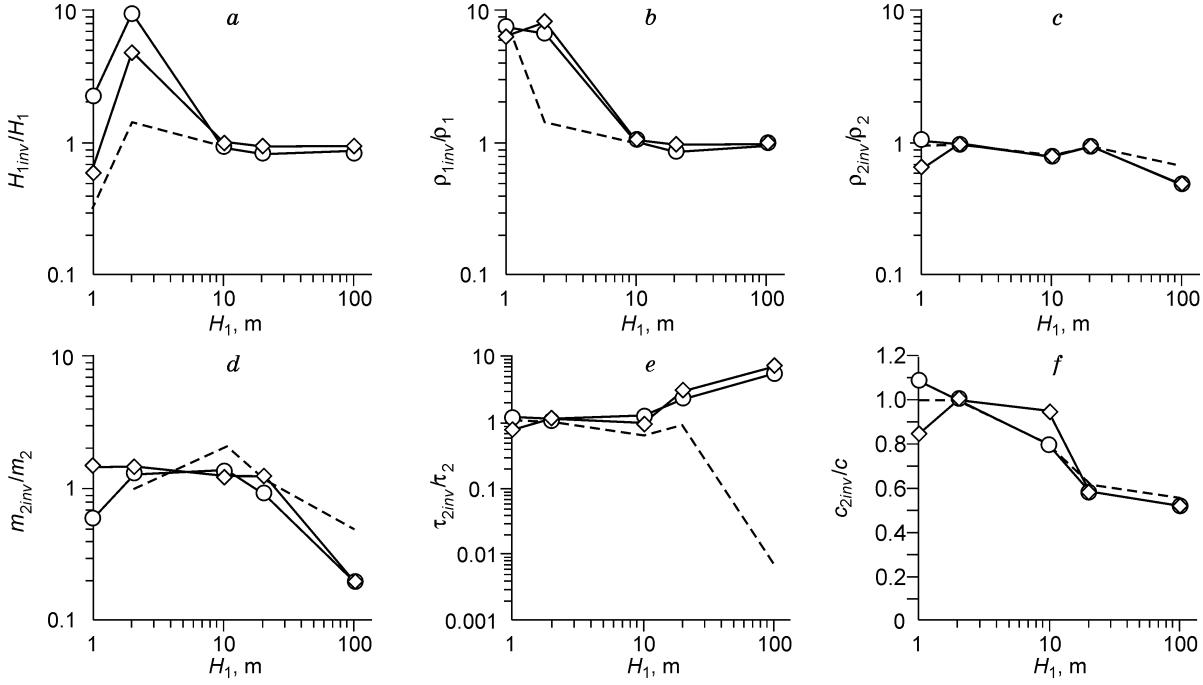

Fig. 5. Parameters reproduced in single and joint inversion (Model 2) as a function of thickness H_1: H_{1inv} (*a*), ρ_{1inv} (*b*), ρ_{2inv} (*c*), m_{2inv} (*d*), τ_{2inv} (*e*), c_{2inv} (*f*). Interpreter was aware that polarizable layer was below (Stage 2). Symbols same as in Fig. 2.

Discussion

The numerical experiments have yielded a large body of diverse data which poses a certain problem in discussing them. Having tried various ways, we find it reasonable to discuss the experiments in terms of availability of a priori information.

Inversion without a priori information available

Model 1. Inversion of pseudo-experimental transient responses corresponding to Model 1 led the interpreter to the right conclusion that the upper layer was polarizable, irrespective of its thickness H_1. If the upper layer was thin, its parameters predicted by single inversion showed a poor fit,

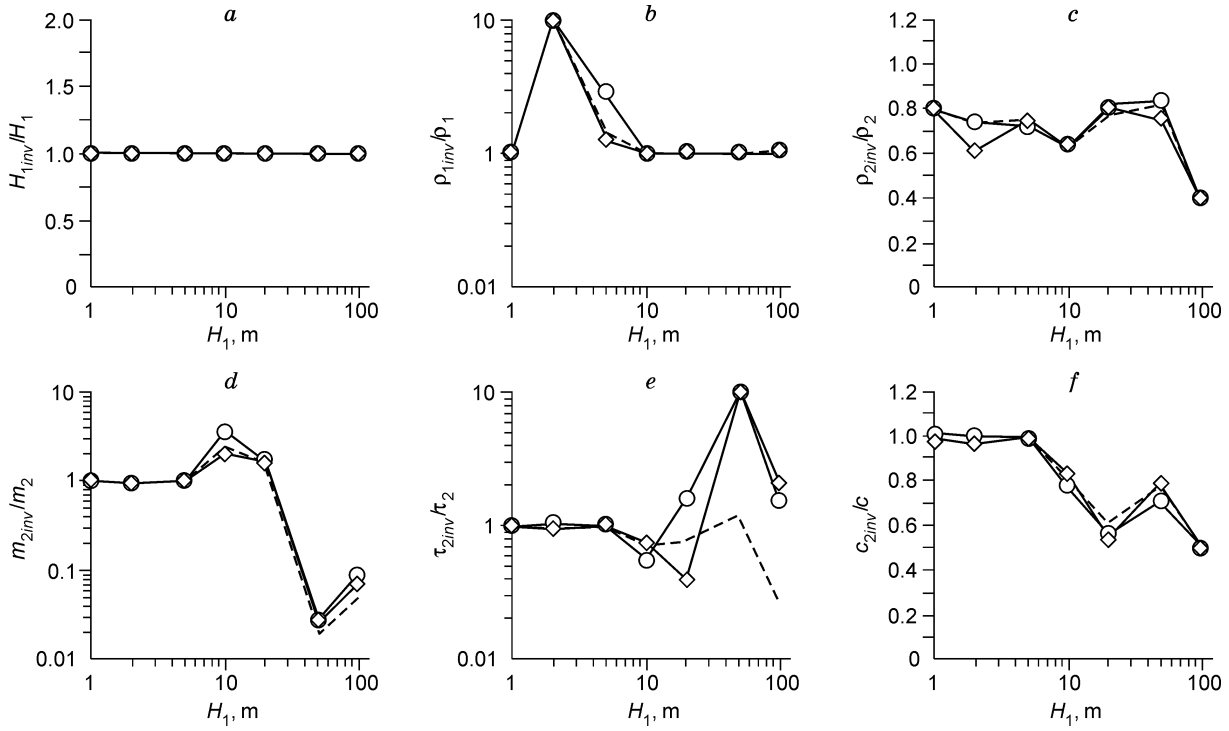

Fig. 6. Parameters reproduced in single and joint inversion of transients with Model 2 as a function of thicknesses H_1: H_{1inv} (*a*), ρ_{1inv} (*b*), ρ_{2inv} (*c*), m_{2inv} (*d*), τ_{2inv} (*e*), c_{2inv} (*f*). In addition to knowledge of model type (Fig. 5), interpreter was aware of assumed layer thicknesses in all models (Stage 3). Symbols same as in Fig. 2.

though the resistivity of the lower layer was reproduced to quite a good accuracy. In the case of a thicker upper layer, the inversion quality was better for its parameters but worse for the lower layer resistivity. Joint inversion definitely improved the fit: it was perfect at H_1 = 5 m or thicker.

This result has important practical implications. Applied to western Yakutia, it means that inversion of TEM data will provide a correct idea of the resistivity and the Cole–Cole parameters of the subsurface with a polarizable upper layer.

Besides the practical value, it is also of general interest. In the case of uniform earth TEM data inversion without a priori information may lead to a two- or three-layer model (Kozhevnikov and Antonov, 2007, 2008). Thus, the two-layer model with a polarizable upper layer turns out to be advantageous over the uniform one in 1D inversion of IP-affected transients. We discussed the reasons for this seemingly unobvious fact in (Kozhevnikov and Antonov, 2009b).

Model 2. All generated transients corresponding to Model 2 with the polarizable layer below were correctly identified as being two-layer earth responses, as in the previous case of Model 1. Yet, they posed a greater problem in recognizing which layer was polarizable: the lower layer was correctly recognized to be polarizable only when the upper layer was thin. In the case of a thicker upper layer, either the upper layer or both layers appeared to be polarizable (Fig. 3, *b*), and the fit of the layer parameters was worse as well.

Although the IP parameters showed a poor fit, the inversion for the layer thickness and resistivity (H_1, ρ_1, and ρ_2) gave satisfactory results: the quality of both single and joint inversion was good at H_1 thicker than a few meters (Fig. 4).

Inversion with a priori information available (Model 2)

The a priori knowledge that just the lower layer was polarizable (Stage 2), eliminated the problem of identifying the starting assumption. As for the estimates of the parameters, the regularity was the same as above. Namely, if the upper layer was thin, the inversion quality was low for its parameters and high for those of the lower layer while in the case of a thick upper layer the situation was opposite (Fig. 5). Note that additional information on the upper layer thickness (Stage 3) did not improve much the fit (Fig. 6).

The dependence of the inversion quality on the upper layer thickness is easy to explain: The thicker the layer the greater its contribution to the total transient response and, correspondingly, the better the fit of its parameters. As for the lower layer, its contribution to the transient response is inversely proportional to its depth and the fit is thus better if it is shallower, i.e., at smaller H_1.

The "disparity" between the two basic models is worth of special comment. It consists in the fact that the models of group 1 are unambiguously recognized as those of a polarizable upper layer upon a nonpolarizable one even in the absence of a priori information, at any thickness H_1, and the fit of the parameters is good; the features of Model 2, on the contrary, are hard to identify without a priori information as those of a polarizable lower layer, and a good inversion quality

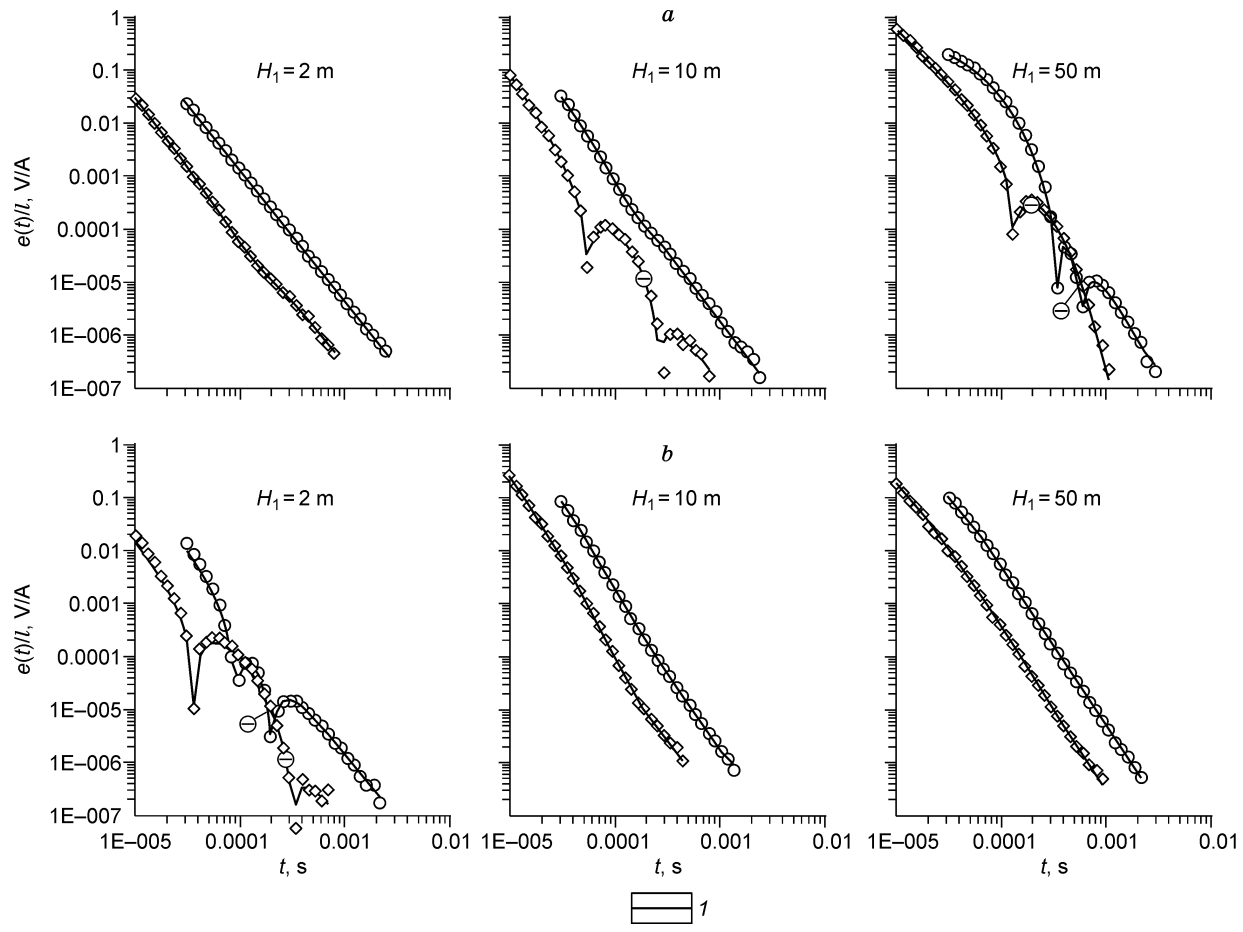

Fig. 7. Pseudo-experimental transients and those obtained through joint inversion of transients corresponding to Models 1 (*a*) and 2 (*b*), without a priori knowledge. Circled minus marks a negative parts of responses. *1*, model transient. Symbols same as in Fig. 2.

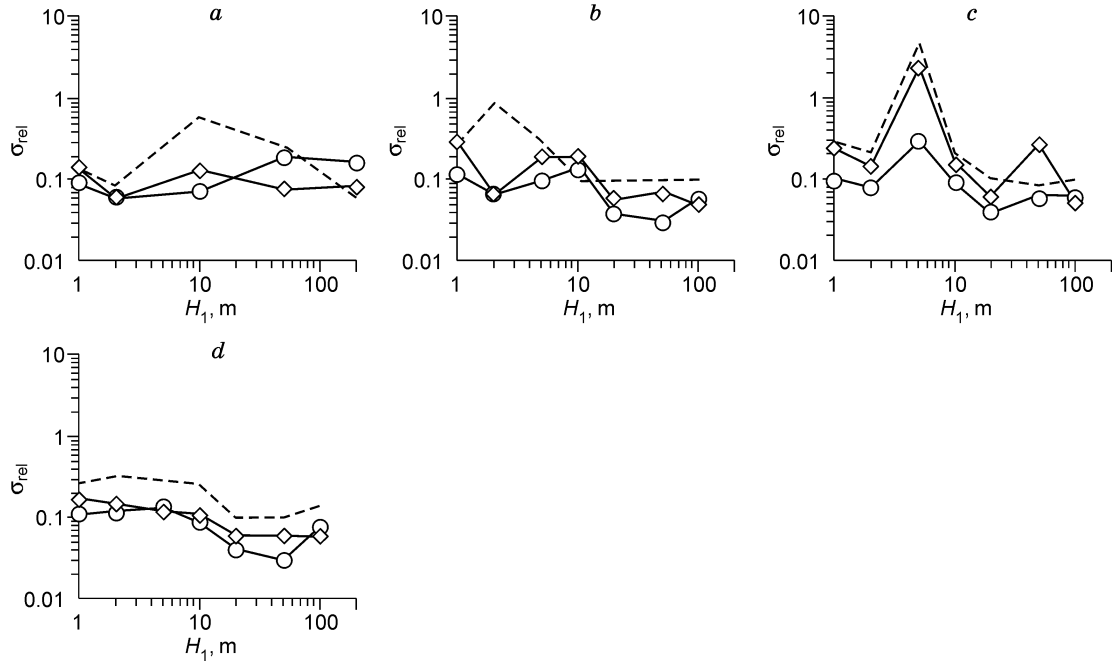

Fig. 8. Relative standard error as a function of thickness H_1. *a*: Model 1, without a priori information; *b–d*: Model 2: stage 1 (*b*), stage 2 (*c*), stage 3(*d*). Symbols same as in Fig. 2.

is achievable only if the upper layer is thin. A conducting upper layer is known to act as a low-frequency filter on the responses from buried structures (West and Macnae, 1991). Its effect in the time domain is to make the response of the polarizable lower layer diffused and shifted toward later times. This leads to overestimated relaxation times and underestimated exponents relative to their true values (Fig. 3). Yet, the low-frequency filter causes no influence on the response of the overlying polarizable layer, which makes Model 1 advantageous over Model 2 in inversion of IP-affected transients. See, for instance, the two models compared in Fig. 7 showing clearly that IP effects become more prominent in Model 1 and less prominent in Model 2 as H_1 increases.

In Figure 8 the relative rms error σ_{rel} (difference between the pseudo-experimental and fitted transients) is plotted as a function of H_1 for Models 1 and 2. In the case of Model 1 (Fig. 8, *a*), the relative error representing the quality of single inversion does not depend on H_1, while the results of joint inversion allow no indefinite judgment on this dependence. In the case of Model 2 (Fig. 8, *b–d*), both single and joint inversion show a trend of σ_{rel} decrease as H_1 increases. Inasmuch as the uncertainty in the lower layer parameters ever increases with growing H_1, σ_{rel} obviously cannot be the only criterion for the model choice. This is especially clear in view of the fact that mean σ_{rel} in joint inversion of Model 2 transients is times greater than that in single inversion (Fig. 8, *b–d*), whereas joint inversion markedly improved the results in most of cases. Thus, it is essential to find other criteria in addition to σ_{rel} that would provide better search for an optimal model when inverting IP-affected transients.

Conclusions

Exploring the potentialities and the limitations of the inversion of IP-affected transients is an urgent problem in present TEM surveys. In this study we have tried to solve it with a numerical experiment in which we inverted in-loop and coincident-loop synthetic transient responses of a two-layer earth consisting of a polarizable layer above (Model 1) or below (Model 2) a nonpolarizable layer. Model 1 showed to be advantageous over Model 2 in TEM applications and gave a good fit of the Cole–Cole parameters (chargeability, IP time constant, and exponent) even in the absence of a priori information. In the case of Model 2, the lack of a priori information caused problems as to recognize which layer was polarizable, and the fit of the Cole–Cole parameters was generally worse. The layer thickness and resistivity estimates were rather accurate in both models, irrespective of whether a priori information was available.

As the upper layer increased in thickness (H_1), the fit of its parameters ever improved in both groups of models while the parameters of the lower layer, on the contrary, contained a greater error. Joint inversion of in-loop and coincident-loop transients improved the fit in the greatest number of cases, i.e., the parameters derived from joint inversion were closer to the true ones.

Relative rms error (σ_{rel}) did not depend on the upper layer thickness for Model 1 but decreased as H_1 increased in the case of Model 2. The error in joint inversion was times that in single inversion, which means that additional criteria other than σ_{rel} may be useful to estimate the inversion quality.

Acknowledgements

The study was supported by grant 07-05-00305 from the Russian Foundation for Basic Research.

References

Artemenko, I.V., Kozhevnikov, N.O., 1999. Modeling the Maxwell–Wagner effect in porphyric frozen ground. Kriosfera Zemli III (1), 60–68.

Kamenetskii, F.M., Sidorov, V.A., Timofeev, V.M., Yakhin, A.M., 1990. TEM processes in conducting polarizable earth, in: Kamenetsky, F.M., Svetov, B.S. (Eds.), Electromagnetic Induction in the Upper Crust [in Russian]. Nauka, Moscow, pp. 14–40.

Karasev, A.P., Shesternev, D.M., Olenchenko, V.V., Yuditskikh, E.Yu., 2004. Modeling fast electrochemical transient processes in frozen ground. Kriosfera Zemli VIII (1), 40–46.

Kozhevnikov, N.O, Artemenko, I.V., 2004. Modeling the effect of dielectric relaxation in frozen ground on ungrounded-loop transient responses. Kriosfera Zemli VIII (2), 30–39.

Kozhevnikov, N.O., Antonov, E.Y., 2006. Fast-decaying IP in frozen unconsolidated rocks and potentialities for its use in permafrost-related TEM studies. Geophysical Prospecting 54, 383–397.

Kozhevnikov, N.O., Antonov, E.Y., 2007. Fast-decaying IP in unconsolidated frozen ground: An inversion numerical experiment for a uniform polarizable earth. Geofizika, No. 1, 42–50.

Kozhevnikov, N.O., Antonov, E.Yu., 2008. Inversion of TEM data affected by fast-decaying induced polarization: Numerical simulation experiment with homogeneous half-space. J. Appl. Geophys. 66, 31–43.

Kozhevnikov, N.O., Antonov, E.Yu., 2009a. Joint inversion of IP-affected TEM data. Russian Geology and Geophysics (Geologiya i Geofizika) 50 (2), 136–142 (181–190).

Kozhevnikov, N.O., Antonov, E.Yu., 2009b. TEM soundings of polarizable earth. Geofizicheskii Zhurnal 31 (4), 104–118.

Kozhevnikov, N.O., Nikiforov, S.P., Snopkov, S.V., 1995. Fast-decaying IP polarization in frozen ground. Geoekologiya, No. 2, 118–126.

Krylov, S.S., Bobrov, N.Yu., 2002. Induction soundings in frozen ground with frequency dependent conductivity. Kriosfera Zemli VI (3), 59–68.

Mityukhin, S.I., 1985. Geological nature of sign-variable transitional processes in Western Yakutia. Geologiya i Geofizika (Soviet Geology and Geophysics) 26 (1), 103–106 (93–95).

Molchanov, A.A., Sidorov, V.A. (Eds.), 1985. Polarization of Rocks [in Russian]. Moscow, VINITI Reports, No. 5847–85.

Molchanov, A.A., Sidorov, V.A., Nikolaev, Yu.V., Yahin, A.M., 1984. New types of transient processes. Izv. AN SSSR, Fizika Zemli, No. 1, 100–103.

Nelder, J.A., Mead, R., 1965. A simplex method for function minimization. Computer Journal 7, 308–313.

Olenchenko, V.V., Kozhevnikov, N.O., Matrosov, V.A., 1978. Fast-decaying IP polarization in frozen ground in the upper section of the Mirnoye kimberlite field, in: Proc. 3rd Saint Petersburg International Conference Exhibition, 7–10 April 2008. Lenexpo, St. Petersburg.

Pelton, W.H., Ward, S.H., Hallof, P.G., Sill, W.R., Nelson, P.H., 1978. Mineral discrimination and removal of inductive coupling with multifrequency IP. Geophysics 43, 588–609.

Shesternev, D.M., Karasev, A.P., Olenchenko, V.V., 2003. Electromagnetic Surveys in Frozen Ground by the Early Induced-Polarization (EIP) Method. Izd. SO RAN, Novosibirsk.

Sidorov, V.A., 1985. Time Domain Electromagnetic Prospecting Methods [in Russian]. Nedra, Moscow.

Sidorov, V.A., 1987. On electrical chargeability of nonuniform rocks. Izv. AN SSSR, Fizika Zemli, No. 10, 58–64.

Stognii, V.V., 2008. TEM method in studies of frozen ground in the Yakutsk kimberlite province. Kriosfera Zemli XII (4), 46–56.

Svetov, B.S., Ageev, V.V., Lebedeva, N.A., 1996. Polarizability of rocks and high-resolution resistivity surveys. Geofizika, No 4, 42–52.

Wait, J.R., 1982. Geo-Electromagnetism. Academic Press, NY.

West, G.F., Macnae, J.C., 1991. Physics of the electromagnetic induction exploration method, in: Nabighian, M.N. (Ed.), Electromagnetic Methods in Applied Geophysics. Vol. 2. Applications, Part A. SEG, pp. 4–45.

Zadorozhnaya, V.Yu., Lepeshkin, V.P., 1998. Induction soundings of IP-affected layered earth. Izv. RAN, Fizika Zemli, No. 4, 55–61.

Zhandalinov, V.M., 2005. TEM Method in Studies of Kimberlite Fields of Western Yakutia [in Russian]. Authors' Abstract, Candidate Thesis. IGF SO RAN, Novosibirsk.

Editorial resposibility: M.I. Epov